Electronic Supplementary Material (ESI) for ChemComm.
This journal is © The Royal Society of Chemistry 2020

SUPPLEMENTARY INFORMATION

Planar or Tetrahedral? A Ternary 17-Electron $CBe_5H_4^+$ Cluster with Planar Pentacoordinate Carbon†

Jin-Chang Guo,‡[a] Lin-Yan Feng,‡[a] Jorge Barroso,[b] Gabriel Merino,*[b] and Hua-Jin Zhai*[a]

[a] *Nanocluster Laboratory, Institute of Molecular Science, Shanxi University, Taiyuan 030006, China*

[b] *Departamento de Física Aplicada, Centro de Investigación y de Estudios Avanzados, Unidad Mérida, km 6 Antigua carretera a Progreso, Apdo. Postal 73, Cordemex, 97310, Mérida, Yuc., México*

*E-mail: gmerino@cinvestav.mx; hj.zhai@sxu.edu.cn

‡ These authors contributed equally to this work.

Molecular dynamics

Table S1. Orbital composition of the HOMOs of C_{2v} CBe_5X_4 (X = K, Au, H, Cl) clusters. Main components are shown in bold.

Table S2. Orbital composition of the HOMOs of C_{3v} CBe_5X_4 (X = K, Au, H, Cl) clusters. Main components are shown in bold.

Table S3. Calculated ionization potentials (IPs; in eV) of neutral CBe_5X_4 (X = K, Au, H, Cl) clusters at the B3LYP/def2-TZVP level, for both their ppC and thC structures.

Table S4. Cartesian coordinates for optimized structures (**1**, **2**, **1′**, and **2′**) of $CBe_5H_4^+$ and CBe_5H_4 clusters at the B3LYP/def2-TZVP level.

Figure S1. Optimized structures of the **1** (C_{2v}, $^2A_1$) global minimum (GM) for $CBe_5H_4^+$ cluster and seven lowest-lying isomers at the B3LYP/def2-TZVP level. Also labeled is isomer **2′** (C_{3v}, $^2A_1$), the neutral counterpart of which is the GM for CBe_5H_4 cluster. Relative energies are listed in kcal mol^{-1} at single-point CCSD(T)//B3LYP/def2-TZVP level with zero-point energy (ZPE) corrections at B3LYP. To ensure the energetics, complementary calculations are also done for structures **1**/**2′** at the B3LYP-D3/def2-TZVP, PBE0/def2-TZVP, and PBE0-D3/def2-TZVP levels, followed by single-point CCSD(T) calculations and ZPE corrections, which yield the CCSD(T) energies of 54.48, 54.51, and 54.51 kcal mol^{-1} for structure **2′**, respectively, as compared to 54.46 kcal mol^{-1} at CCSD(T)//B3LYP. Shown in *italic* (the second line) are selected energetics data at single-point CCSD(T)/def2-TZVP//PBE0-D3/ def2-TZVP level for all eight lowest-lying structures. This paper will primarily discuss the B3LYP and single-point CCSD(T)//B3LYP data.

Figure S2. Optimized structures of **1′** (C_{2v}, $^1A_1$) for neutral CBe_5H_4 cluster and **2′** (C_{3v}, $^2A_1$) for $CBe_5H_4^+$ at the B3LYP/def2-TZVP level. Bond distances (in Å) and natural atomic charges (in |e|; red color) are shown. Structures **1′** and **2′** are 5.85 and 61.66 kcal mol^{-1} above **2** and **1**, respectively, at the B3LYP level with ZPE corrections. These values are refined to 10.32 and 54.46 kcal mol^{-1} at single-point CCSD(T) level with ZPE corrections at B3LYP.

Figure S3. Dimerization of GM C_{2v} $CBe_5H_4^+$ (**1**) cluster. (a) Optimized C_{2h} (^1A_g) geometry of $(CBe_5H_4)_2^{2+}$ cluster at the B3LYP/def2-TZVP level, which is a true minimum. Cohesive energy for the reaction is **−**10.40 kcal mol^{-1} at B3LYP. (b) Chemical

bonding scheme for C_{2h} $(CBe_5H_4)_2^{2+}$ cluster according to the adaptive natural density partitioning (AdNDP) analysis. Occupation numbers (ONs) are shown.

Figure S4. Calculated nucleus independent chemical shifts (NICSs) for the series of neutral CBe_5X_4 (X = K, Au, H, Cl) clusters and their cation counterparts. NICS(1) values, calculated at 1 Å above the triangles and ppC centers, are shown in red and NICS(0) in blue. Qualitatively, NICS(1) reflects π aromaticity, whereas NICS(0) is largely associated to σ aromaticity.

Figure S5. Root-mean-square deviations (RMSD) of the ppC and thC structures of $CBe_5H_4^+$ during Born-Oppenheimer molecular dynamics (BOMD) simulations. (a) At room temperature (298 K), C_{3v} thC isomer **2′** undergoes structural change and converts to ppC structure **1** within less than 2 ps. (b) C_{2v} ppC GM structure **1** is dynamically robust at 398 K (well beyond room temperature).

Figure S6. Canonical molecular orbitals (CMOs) of the thC GM structure C_{3v} (**2**) of CBe_5H_4. HOMO–4 through HOMO–6 can be transformed to four tetrahedral C–Be σ single bonds, and HOMO–1 through HOMO–3 are responsible for four Be–H σ single bonds. HOMO is primarily associated to Be–Be σ single bond and yet with substantial H–Be–Be–C σ conjugation; see Figure 4.

Figure S7. Orbital energy level diagrams of isomer ppC C_{2v} (**1′**) (right) and GM thC C_{3v} (**2**) (left) of cluster CBe_5H_4 at the B3LYP/def2-TZVP level.

Figure S8. Optimized thC and ppC structures of CBe_5X_4 and $CBe_5X_4^+$ (X = K, Au, Cl) at the B3LYP/def2-TZVP level, along with their relative energies in kcal mol^{-1} at this level. Bond distances (in Å) and natural atomic charges (in |e|; red color) are shown.

Molecular dynamics

Is cluster **1** dynamically robust as well? Our Born-Oppenheimer molecular dynamics (BOMD) simulations at 298 and 398 K support its dynamic stability. As shown in Fig. S5 (ESI†), the species is stable at 398 K (well above room temperature; Fig. S5b) and maintains its ppC structure during the 20 ps simulation. In contrast, the thC cation **2′** is dynamically unstable and converts automatically to cluster **1** within less than 2 ps, even at room temperature (298 K; Fig. S5a).

This is understandable because the Be–Be bond in $CBe_5H_4^+$ (**2′**) is 2.37 Å (Fig. S2, ESI†) with a NBO bond order of 0.35 only, which is prone to breakage. Once the Be–Be link in **2′** is broken, the cluster easily reorganizes to its ppC geometry, driven by electrostatics between the negative C and positive Be centers. Thus, thermodynamics and molecular dynamics collectively suggest that cluster **1** as a ppC species is viable and may be detected in gas-phase experiments.

Table S1. Orbital composition of the HOMOs of C_{2v} CBe_5X_4 (X = K, Au, H, Cl) clusters. Main components are shown in bold.

Species	HOMO	Symmetry	Be_5 (%)		X_4 (%)		C (%)	
			s	p	s	p/d	s	p
CBe_5K_4	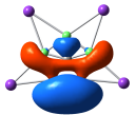	a_1	**32.95**	**57.76**	4.36	1.49	0.49	2.95
CBe_5Au_4	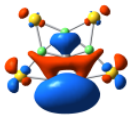	a_1	**38.00**	**51.58**	1.73	3.95	1.77	2.97
CBe_5H_4	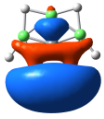	a_1	**50.45**	**44.18**	0.52	0.00	1.78	3.07
CBe_5Cl_4	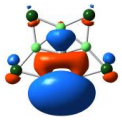	a_1	**46.38**	**43.76**	0.14	3.04	1.59	5.09

Table S2. Orbital composition of the HOMOs of C_{3v} CBe_5X_4 (X = K, Au, H, Cl) clusters. Main components are shown in bold.

Species	HOMO	Symmetry	Be_5 (%)		X_4 (%)		C (%)	
			s	p	s	p/d	s	p
CBe_5K_4		a_1	**23.15**	**38.56**	**36.95**	0.20	0.02	1.12
CBe_5Au_4	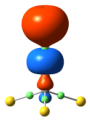	a_1	**12.90**	**30.20**	**48.06**	**6.15**	0.26	2.43
CBe_5H_4	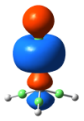	a_1	**36.42**	**42.44**	**14.30**	0.00	0.53	**6.31**
CBe_5Cl_4	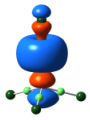	a_1	**49.44**	**37.45**	0.09	3.88	0.55	**8.59**

Table S3. Calculated ionization potentials (IPs; in eV) of neutral CBe_5X_4 (X = K, Au, H, Cl) clusters at the B3LYP/def2-TZVP level, for both their ppC and thC structures.

Species	CBe_5K_4	CBe_5Au_4	CBe_5H_4	CBe_5Cl_4
C_{2v} ppC	3.44	5.76	6.25	6.40
C_{3v} thC	3.68	7.99	9.27	9.71
ΔIP^a	0.24	2.23	3.02	3.31

[a] $\Delta IP = IP(thC) - IP(ppC)$. It characterizes the gain in terms of energetics for the ppC structure upon removal of one electron, that is, the enhancement of stability of ppC isomer with respect to thC for the 17-electron cation system.

Figure S1. Optimized structures of the **1** (C_{2v}, $^2A_1$) global minimum (GM) for $CBe_5H_4^+$ cluster and seven lowest-lying isomers at the B3LYP/def2-TZVP level. Also labeled is isomer **2′** (C_{3v}, $^2A_1$), the neutral counterpart of which is the GM for CBe_5H_4 cluster. Relative energies are listed in kcal mol^{-1} at single-point CCSD(T)//B3LYP/def2-TZVP level with zero-point energy (ZPE) corrections at B3LYP. To ensure the energetics, complementary calculations are also done for structures **1**/**2′** at the B3LYP-D3/def2-TZVP, PBE0/def2-TZVP, and PBE0-D3/def2-TZVP levels, followed by single-point CCSD(T) calculations and ZPE corrections, which yield the CCSD(T) energies of 54.48, 54.51, and 54.51 kcal mol^{-1} for structure **2′**, respectively, as compared to 54.46 kcal mol^{-1} at CCSD(T)//B3LYP. Shown in *italic* (the second line) are selected energetics data at single-point CCSD(T)/def2-TZVP//PBE0-D3/ def2-TZVP level for all eight lowest-lying structures. This paper will primarily discuss the B3LYP and single-point CCSD(T)//B3LYP data.

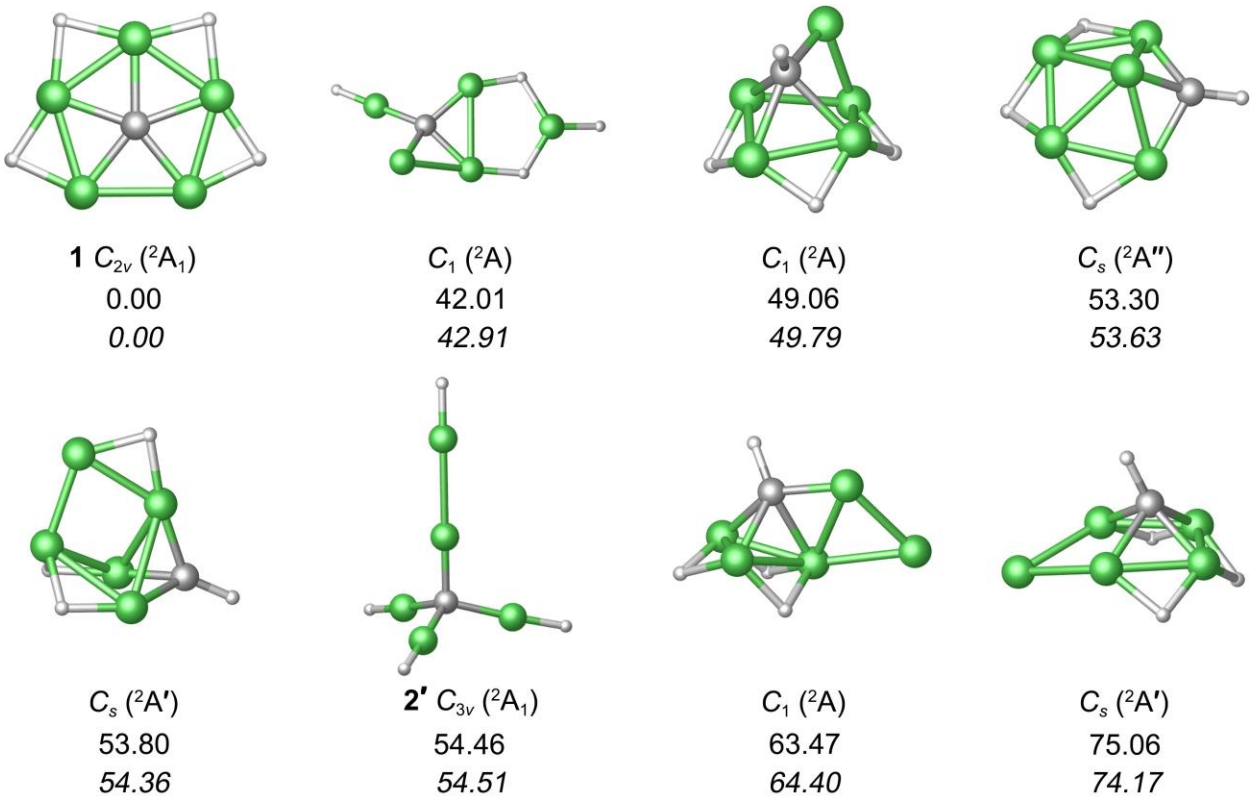

Figure S2. Optimized structures of **1′** (C_{2v}, $^1A_1$) for neutral CBe_5H_4 cluster and **2′** (C_{3v}, $^2A_1$) for $CBe_5H_4^+$ at the B3LYP/def2-TZVP level. Bond distances (in Å) and natural atomic charges (in |e|; red color) are shown. Structures **1′** and **2′** are 5.85 and 61.66 kcal mol^{-1} above **2** and **1**, respectively, at the B3LYP level with ZPE corrections. These values are refined to 10.32 and 54.46 kcal mol^{-1} at single-point CCSD(T) level with ZPE corrections at B3LYP.

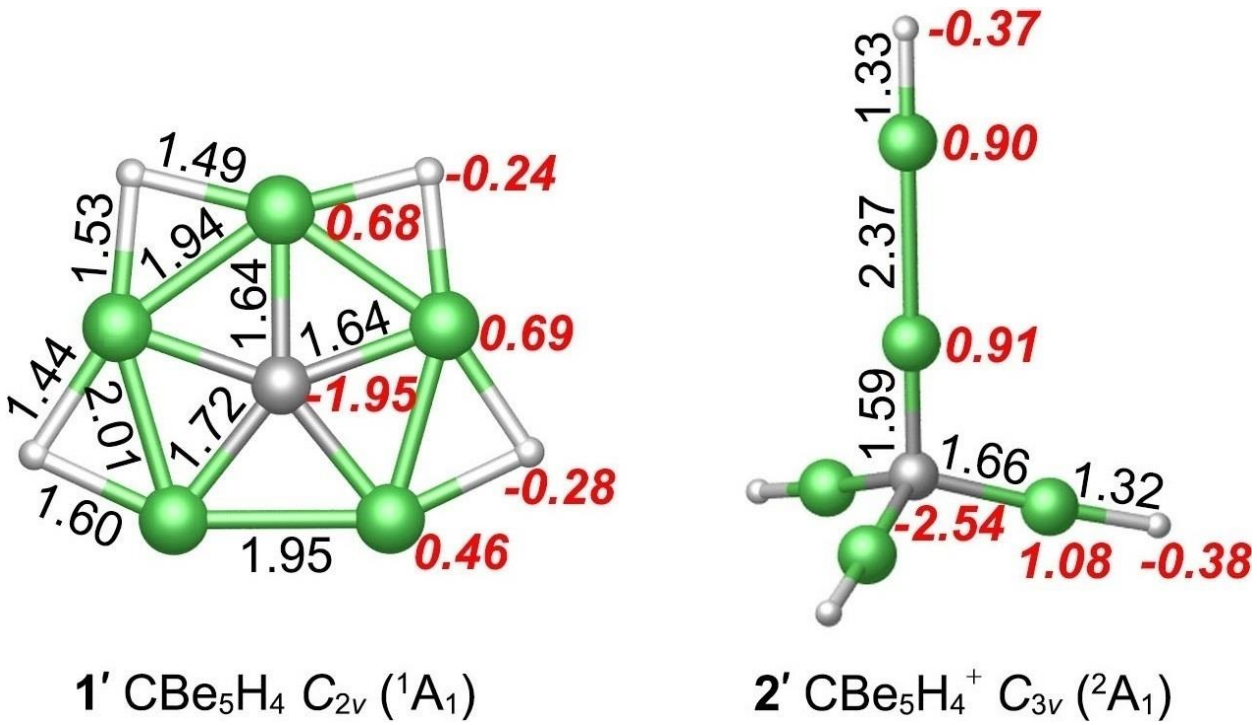

Figure S3. Dimerization of GM C_{2v} $CBe_5H_4^+$ (**1**) cluster. (a) Optimized C_{2h} (^1A_g) geometry of $(CBe_5H_4)_2^{2+}$ cluster at the B3LYP/def2-TZVP level, which is a true minimum. Cohesive energy for the reaction is –10.40 kcal mol^{-1} at B3LYP. (b) Chemical bonding scheme for C_{2h} $(CBe_5H_4)_2^{2+}$ cluster according to the adaptive natural density partitioning (AdNDP) analysis. Occupation numbers (ONs) are shown.

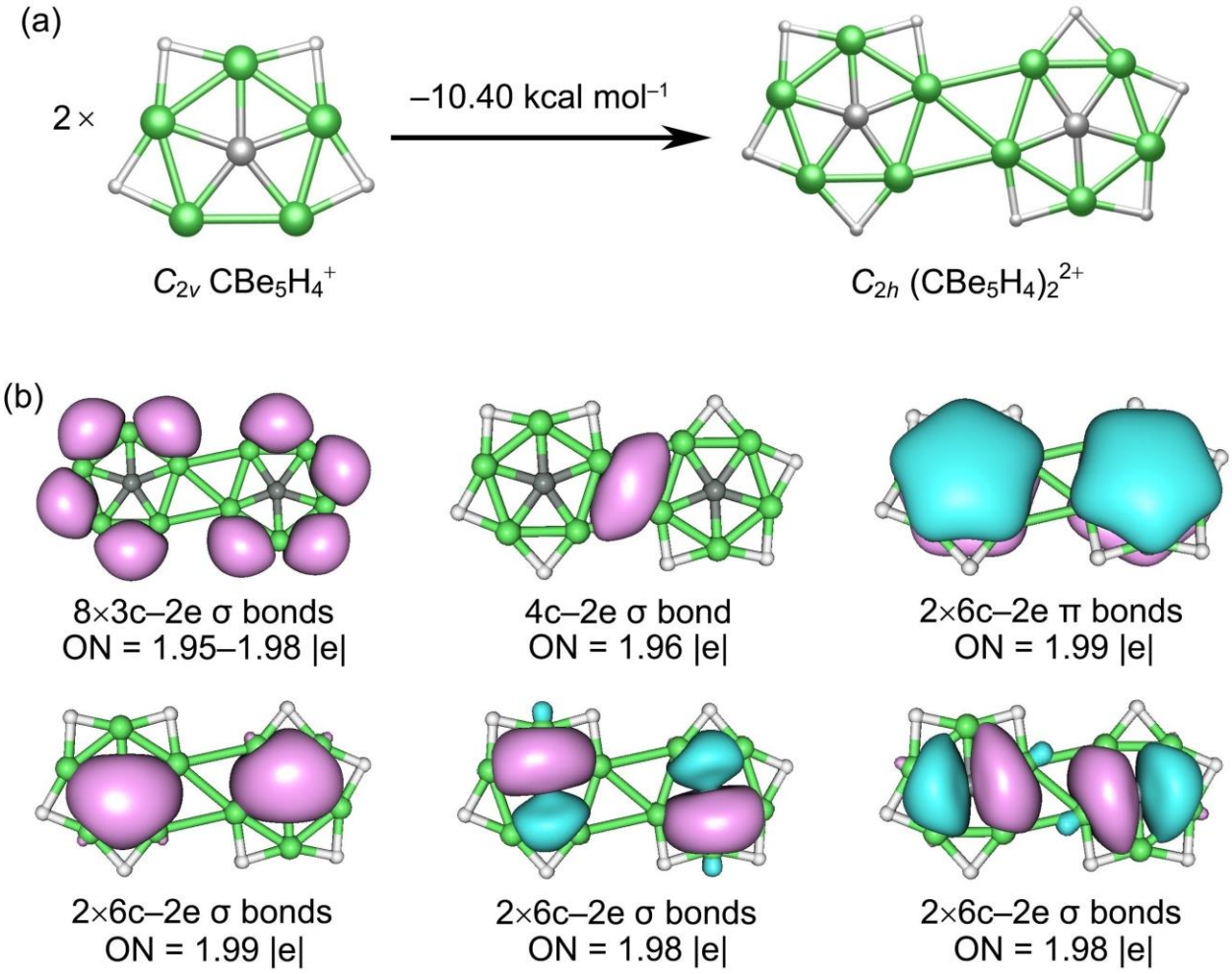

Figure S4. Calculated nucleus independent chemical shifts (NICSs) for the series of neutral CBe_5X_4 (X = K, Au, H, Cl) clusters and their cation counterparts. NICS(1) values, calculated at 1 Å above the triangles and ppC centers, are shown in red and NICS(0) in blue. Qualitatively, NICS(1) reflects π aromaticity, whereas NICS(0) is largely associated to σ aromaticity.

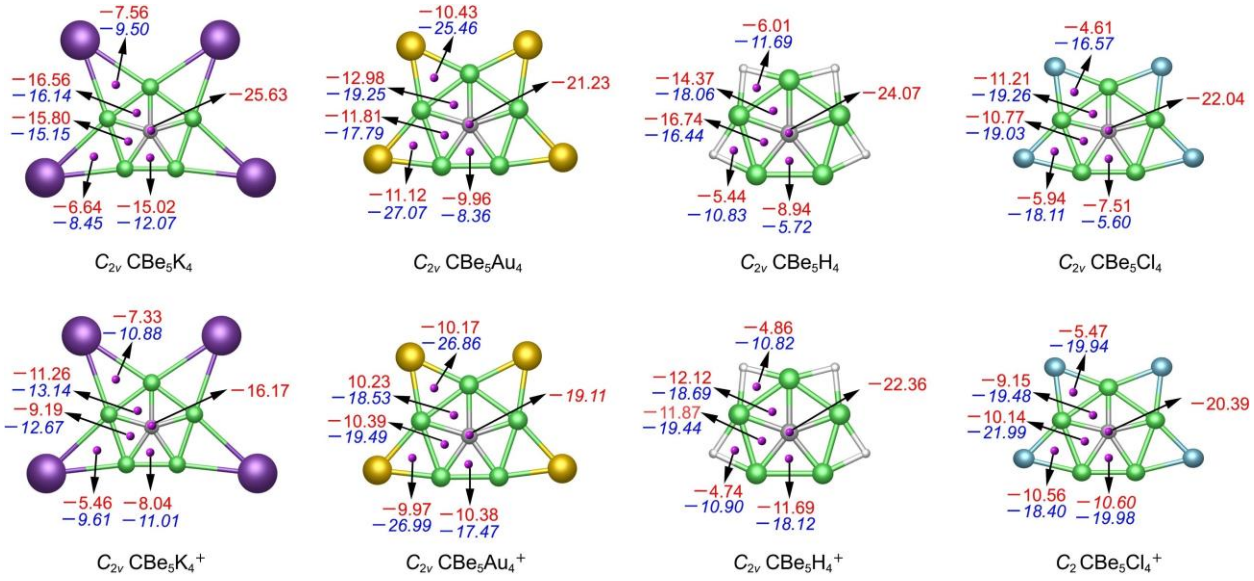

Figure S5. Root-mean-square deviations (RMSD) of the ppC and thC structures of $CBe_5H_4^+$ during Born-Oppenheimer molecular dynamics (BOMD) simulations. (a) At room temperature (298 K), C_{3v} thC isomer **2′** undergoes structural change and converts to ppC structure **1** within less than 2 ps. (b) C_{2v} ppC GM structure **1** is dynamically robust at 398 K (well beyond room temperature).

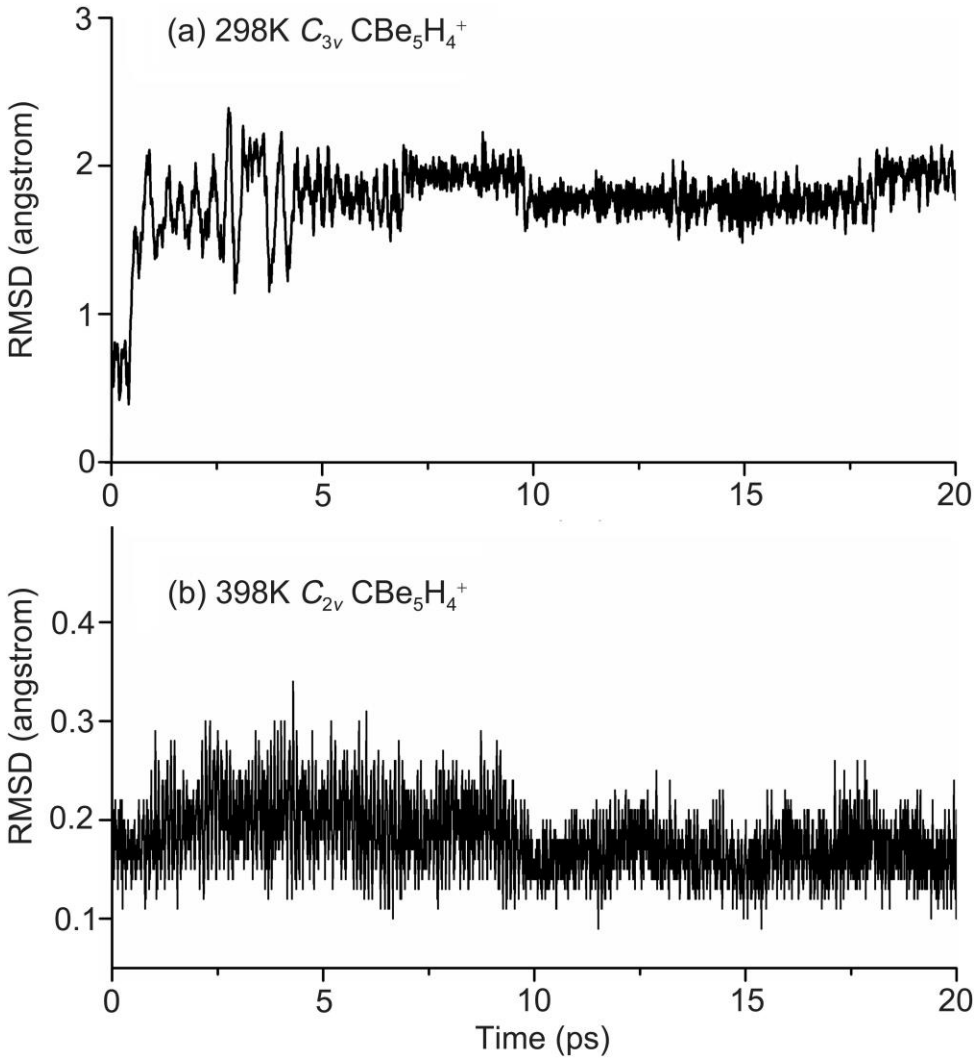

Figure S6. Canonical molecular orbitals (CMOs) of the thC GM structure C_{3v} (**2**) of CBe_5H_4. HOMO–4 through HOMO–6 can be transformed to four tetrahedral C–Be σ single bonds, and HOMO–1 through HOMO–3 are responsible for four Be–H σ single bonds. HOMO is primarily associated to Be–Be σ single bond and yet with substantial H–Be–Be–C σ conjugation; see Figure 4.

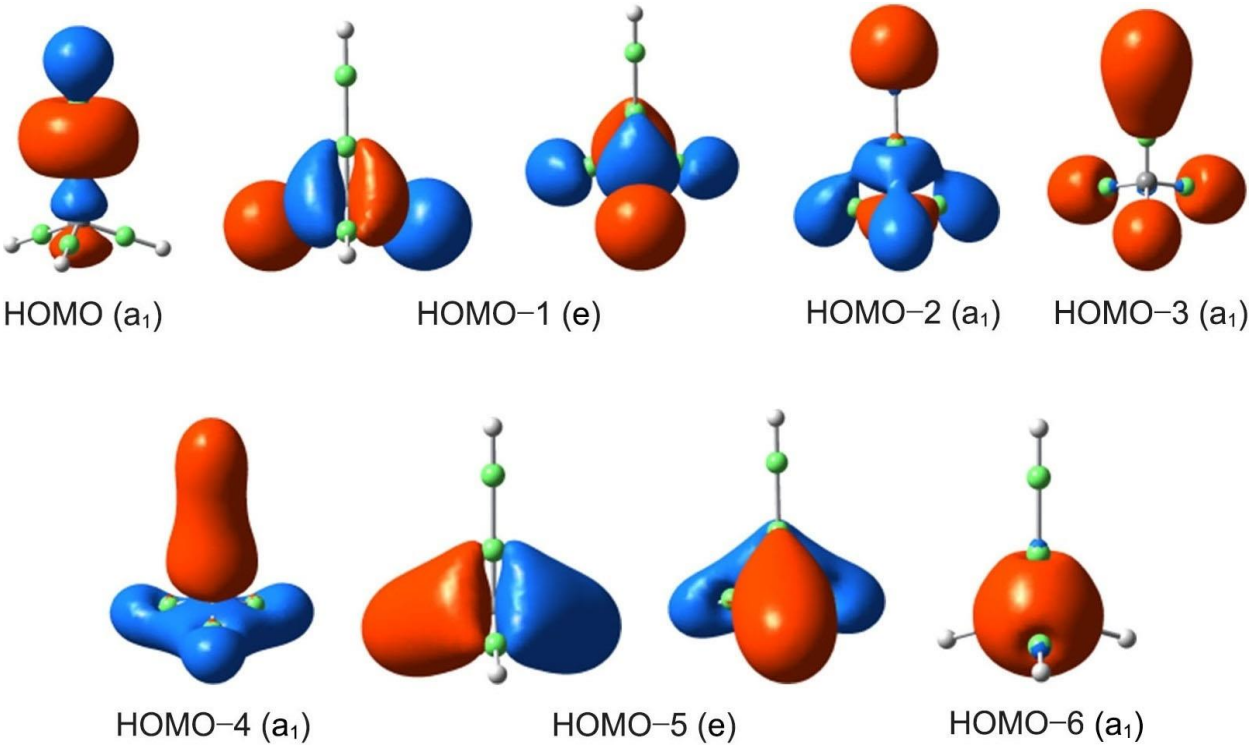

Figure S7. Orbital energy level diagrams of isomer ppC C_{2v} (**1′**) (right) and GM thC C_{3v} (**2**) (left) of cluster CBe_5H_4 at the B3LYP/def2-TZVP level.

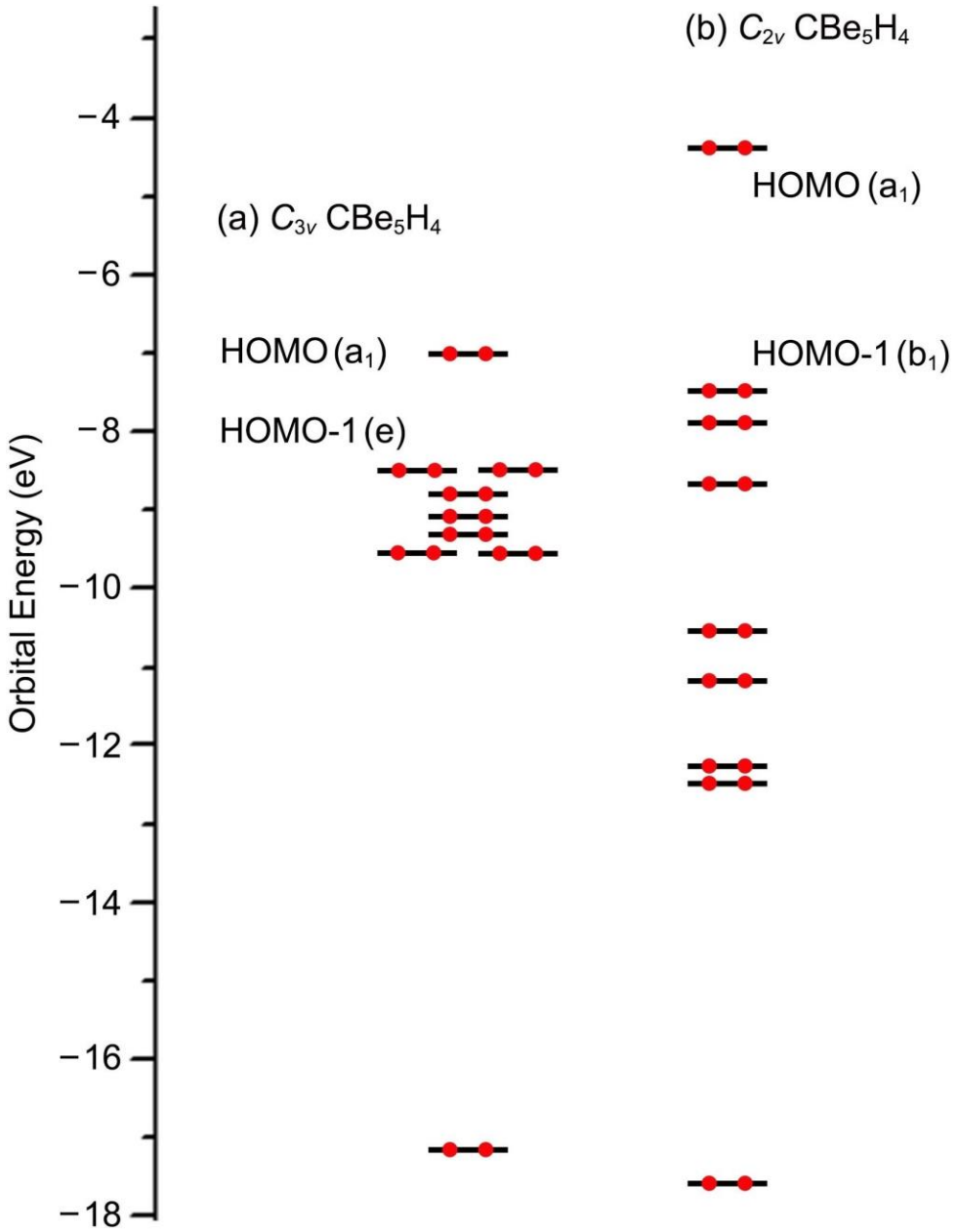

Figure S8. Optimized thC and ppC structures of CBe_5X_4 and $CBe_5X_4^+$ (X = K, Au, Cl) at the B3LYP/def2-TZVP level, along with their relative energies in kcal mol^{-1} at this level. Bond distances (in Å) and natural atomic charges (in |e|; red color) are shown.

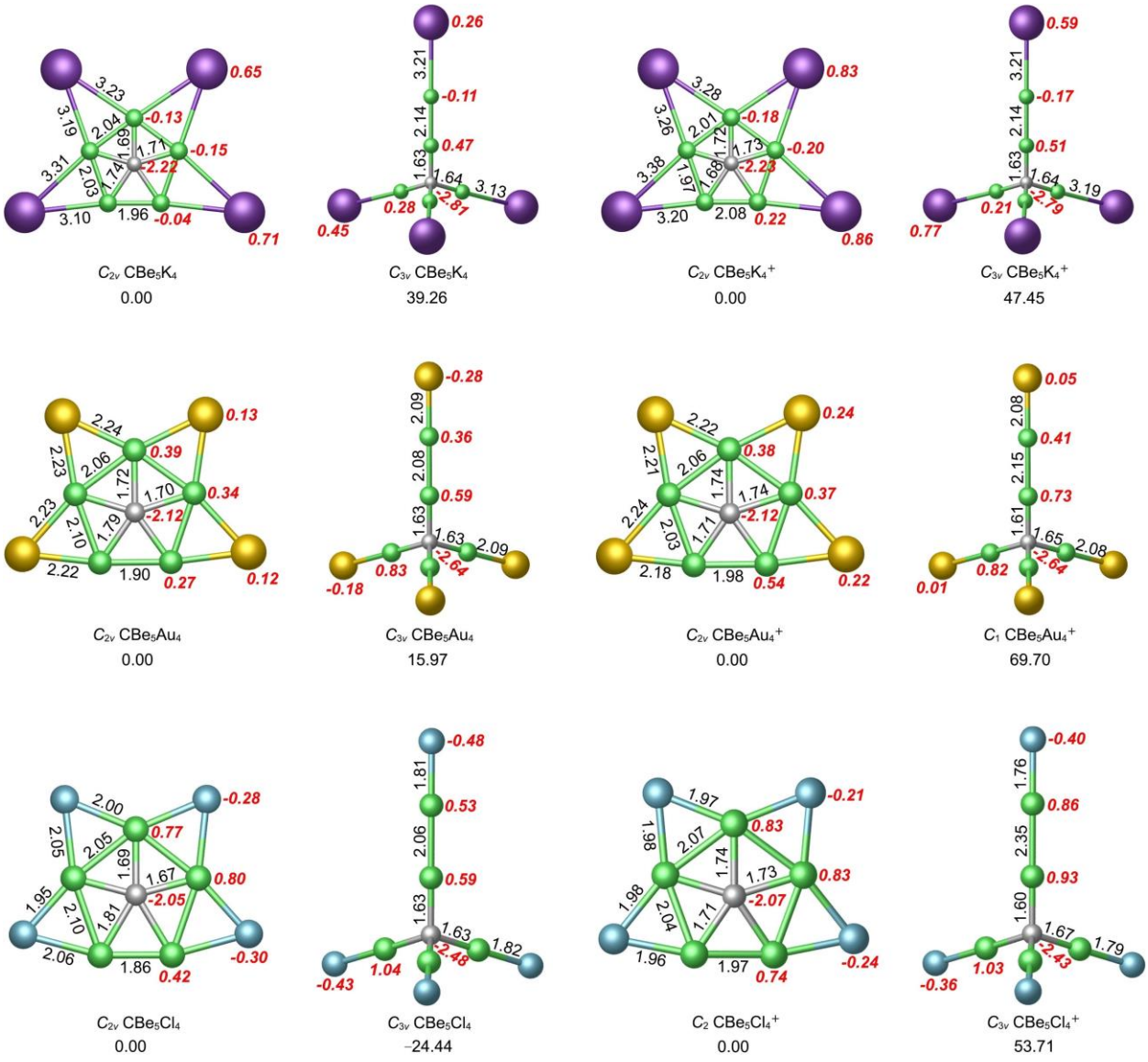

Table S4. Cartesian coordinates for optimized structures (**1**, **2**, **1′**, and **2′**) of $CBe_5H_4^+$ and CBe_5H_4 clusters at the B3LYP/def2-TZVP level.

1 (C_{2v}, $^2A_1$)

	X	Y	Z
C	0.00000000	0.12005400	0.00000000
H	2.39548300	0.78215900	0.00000000
H	-2.39548300	0.78215900	0.00000000
H	-1.43569300	-1.92027900	0.00000000
H	1.43569300	-1.92027900	0.00000000
Be	1.04559700	1.42138400	0.00000000
Be	1.58238300	-0.44499400	0.00000000
Be	-1.04559700	1.42138400	0.00000000
Be	-1.58238300	-0.44499400	0.00000000
Be	0.00000000	-1.56380200	0.00000000

2 (C_{3v}, $^1A_1$)

	X	Y	Z
C	0.00000000	0.00000000	0.56670800
Be	0.00000000	0.00000000	-1.06745300
Be	0.00000000	0.00000000	-3.14673500
H	0.00000000	0.00000000	-4.48434700
Be	0.00000000	1.53358600	1.10887300
H	0.00000000	2.78831800	1.54479200
Be	1.32812500	-0.76679300	1.10887300
H	2.41475400	-1.39415900	1.54479200
Be	-1.32812500	-0.76679300	1.10887300
H	-2.41475400	-1.39415900	1.54479200

1′ (C_{2v}, $^1A_1$)

	X	Y	Z
C	0.00000000	0.06059800	0.00000000
H	2.39216000	0.73930200	0.00000000
H	-2.39216000	0.73930200	0.00000000
H	-1.44058200	-1.95537600	0.00000000
H	1.44058200	-1.95537600	0.00000000
Be	0.97425900	1.48355500	0.00000000
Be	1.56087700	-0.43445400	0.00000000
Be	-0.97425900	1.48355500	0.00000000
Be	-1.56087700	-0.43445400	0.00000000
Be	0.00000000	-1.58106200	0.00000000

2′ (C_{3v}, $^2A_1$)

	X	Y	Z
C	0.00000000	0.00000000	0.63848800
Be	0.00000000	0.00000000	-0.94936200
Be	0.00000000	0.00000000	-3.32155700
H	0.00000000	0.00000000	-4.64902800
Be	0.00000000	1.59023500	1.12869900
H	0.00000000	2.86752500	1.45246200
Be	1.37718400	-0.79511800	1.12869900
H	2.48335000	-1.43376300	1.45246200
Be	-1.37718400	-0.79511800	1.12869900
H	-2.48335000	-1.43376300	1.45246200